Scripta Materialia 135 (2017) 92–96

Contents lists available at ScienceDirect

Scripta Materialia

journal homepage: www.elsevier.com/locate/scriptamat

Regular article

# On the deformation response and cyclic stability of $Ni_{50}Ti_{35}Hf_{15}$ high temperature shape memory alloy wires

D. Canadinc [a], W. Trehern [a], H. Ozcan [b], C. Hayrettin [a], O. Karakoc [a], I. Karaman [a,b,*], F. Sun [c], Z. Chaudhry [c]

[a] Department of Materials Science and Engineering, Texas A&M University, College Station, TX 77843, USA
[b] Department of Mechanical Engineering, Texas A&M University, College Station, TX 77843, USA
[c] United Technologies Research Center, E. Hartford, CT 06108, USA

ARTICLE INFO

*Article history:*
Received 7 February 2017
Received in revised form 19 March 2017
Accepted 21 March 2017
Available online xxxx

*Keywords:*
High temperature shape memory alloys
Martensitic transformation
Training
Superelasticity
NiTiHf

ABSTRACT

The processing - phase transformation - deformation response relationship of $Ni_{50}Ti_{35}Hf_{15}$ high temperature shape memory alloy was studied. As the material was hot extruded and further underwent wire drawing, the phase transformation temperatures decreased and the strength levels increased, yet the initial brittle response was replaced by near-perfect superelastic response above the austenite finish temperature. Moreover, the $Ni_{50}Ti_{35}Hf_{15}$ wires exhibited a remarkably stable cyclic actuation response under 300 MPa, as compared to the poor cyclic stability of the hot extruded samples, which is beyond the operating stress levels for known shape memory actuators.



Shape memory alloys (SMAs), and in particular nickel-titanium (NiTi), continue to be the material of choice in a variety of applications owing to their superior functional properties facilitated by thermo-elastic martensitic transformation [1,2]. However, the current SMAs are not suitable for high temperature applications: NiTi and many NiTi-based SMAs possess martensitic transformation temperatures (TTs) below 100 °C, which warrants the development of high temperature SMAs (HTSMAs) operating at elevated temperatures [2,3]. In order to preserve the superior thermo-mechanical properties of NiTi while increasing the TTs, ternary alloying of NiTi with Pd, Pt and Au has proven successful [2]. However, the high cost of these ternary elements led the SMA community to seek other alternatives, and Ni-rich ternary alloys containing Hf or Zr have recently gained significant attention [3–18]. Specifically, the NiTiHf alloys with less than 25 at.% Hf undergo B2-to-B19′ martensitic transformation similar to NiTi [19], and a Hf content of more than 10 at.% leads to a significant increase in TTs [2]. Consequently, NiTiHf HTSMAs containing 10–20 at.% Hf have received recent interest [2,4–13,16–18,20,21], and the thermo-mechanical and shape memory characteristics of the Ni-rich NiTiHf alloys have been well established.

One important obstacle against the utility of NiTiHf alloys in practical forms is the fact that the reversible martensitic transformation in stoichiometric or Ti-rich alloys is relatively poor [2,15]. This obstacle demands modifications of the microstructure in order to control or suppress plastic deformation that deteriorates the reversibility of martensitic transformation. However, there is a very limited volume of work on the thermo-mechanical processing, grain size refinement, and work hardening of HTSMAs, in particular NiTiHf [15,22] that would improve the reversibility of the transformation. Their B2 structure in austenite, and thus inherent brittleness, sensitivity to carbon and oxygen impurities, and carbide or oxide formation leads to the difficulty of processing of these materials. The Ni-rich compositions can form nano-precipitates and exhibit more stable reversible martensitic transformation [4,20,21], however; the excess Ni increases the strength and make these alloys more brittle, hindering Ni-rich alloys to be formed into different forms [2].

Consequently, the focus has been limited to the characterization of standard laboratory samples in single- or polycrystalline forms of NiTiHf alloys, and to the best of the authors' knowledge, shape memory characteristics of these alloys in practical forms, particularly as wires, have not been explored. The work presented herein was undertaken with the aim of addressing this issue: we report on the temperature and training dependent tensile response of a NiTiHf HTSMA, which was studied in the form of a 0.75 mm diameter wire. Even though NiTi SMA wires have been studied to assess their utility for various applications [23–30], the present work constitutes the first report on the thermo-mechanical characterization of NiTiHf HTSMA wires, which are promising candidates for several aerospace applications, including the active clearance control in jet propulsion engines [2]. Since such applications necessitate superior actuation response and cyclic stability, we also report on

* Corresponding author at: Department of Materials Science and Engineering, Texas A&M University, College Station, TX 77843, USA.
*E-mail address:* ikaraman@tamu.edu (I. Karaman).

http://dx.doi.org/10.1016/j.scriptamat.2017.03.025
1359-6462/

the actuation response and thermo-mechanical cyclic stability of the NiTiHf HTSMA wires.

For this purpose, a NiTiHf alloy with a nominal composition of $Ni_{50}Ti_{35}Hf_{15}$ (at.%) was studied. The stoichiometric $Ni_{50}Ti_{35}Hf_{15}$ alloy was chosen in order to avoid the aforementioned difficulties related to the processing of non-stoichiometric compositions. The material was initially fabricated into the 200 mm long as-cast and hot isostatic pressed cylindrical bars with a diameter of 12.7 mm. The wires were obtained by further hot extrusion of these bars followed by the subsequent wire drawing. In order to assure that the intermediate processing step (hot extrusion) has been successfully completed, the thermo-mechanical properties of the hot-extruded material were also studied and reported.

The TTs of the samples were determined using differential scanning calorimetry (DSC) with a heating/cooling rate of 10 °C/min. The dogbone shaped samples with the gage section of 3 mm × 8 mm × 1.5 mm were cut from the initial $Ni_{50}Ti_{35}Hf_{15}$ bars using wire electrical discharge machining (EDM), and then deformed under tensile loading with a strain rate of $1 \times 10^{-4}$ $s^{-1}$ on a servohydraulic MTS test frame equipped with a high-temperature extensometer. The thermo-mechanical cycling/training of the bulk samples was carried out on 95 mm long flat dog-bone shaped tensile specimens with 1 mm thickness, 40 mm length, and 2.5 mm width in the gage section, which were also cut from the initial bars using wire EDM. During the thermo-mechanical cycling, electric current was passed through the specimens to heat them above the austenite finish temperature ($A_f$), and cooling down to below martensite finish temperature ($M_f$) was achieved through convection utilizing a slow speed electric fan.

Prior to wire drawing, the 200 mm long $Ni_{50}Ti_{35}Hf_{15}$ bars were further hot extruded with a 6.35:1 reduction in diameter to obtain 1.5 m long and 2 mm diameter wires. This hot extrusion was carried out at 900 °C and in two steps, such that a 2:1 diameter reduction was imposed during the first step, and the intermediate product was then separately hot extruded down to a final diameter of 2 mm. The materials were sealed in stainless steel jackets to prevent oxidation during the hot extrusion. The final product of 2 mm $Ni_{50}Ti_{35}Hf_{15}$ wires were deformed under tensile loading on an electro-mechanical test setup equipped with special grips and a laser extensometer.

Final wire drawing was carried out in five steps, and the output of each step was furnace annealed at 700 °C in argon to yield a final product of 12 m long and 0.75 mm diameter wire. The quality of the $Ni_{50}Ti_{35}Hf_{15}$ wires was monitored utilizing a FEI Quanta 600 scanning electron microscope (SEM) prior to the experiments, assuring the absence of any undesired cracks or flaws that would deteriorate the properties during the training. Energy-dispersive X-ray spectroscopy (EDX) was carried out on the as-is bulk, hot extruded 2 mm wire and the 0.75 mm wire samples in order to reveal the compositional differences between the observed particles and the matrix after each processing step. Furthermore, the average size of the particles in the initial bulk, hot extruded 2 mm wire and the 0.75 mm wire samples were measured.

In order to evaluate the cyclic stability of the actuation response and determine the role of training on the resulting mechanical properties, the 0.75 mm wires were thermo-mechanically cycled/trained for 200 cycles under 300 MPa constant stress utilizing the custom-built SMA thermo-mechanical cycling setup. The chosen stress level of 300 MPa is beyond the operating stress levels for many SMA actuators, while 200 cycles was selected in order to assess the effects of cycling at early stages. Utilizing the thermo-mechanical cycling setup, 200 mm long wire samples were heated up by Joule heating with a programmable power source, and the voltage and data acquisition were controlled by a Labview program. Temperature was measured using K-type thermocouples connected to a data acquisition board, while the displacement was measured using a laser displacement sensor. The input voltage and current remained below 4 V and 5 A, respectively, under the applied direct current. 60 mm long samples were then cut from the trained wires, and they were tested on a screw-driven MTS test frame equipped with a laser extensometer and special grips for wire testing.

The initial tensile test results showed that the initial bulk material exhibited relatively low ductility of about 5% strain (Fig. 1) when deformed at $M_f$ (170 °C, Fig. 2), while loading at 10 °C above the $A_f$, i.e. 270 °C, led to a constant-stress plateau up to 8% strain and 3.2% superelastic strain upon unloading. After the hot extrusion, the resulting 2 mm wires were still brittle under tension in martensite and the wires failed at about 5.4% strain at 170 °C. However, the strength levels attained at the failure were about two-fold higher as compared to the bulk material (Fig. 1), although the TTs decreased by only about 10–15 °C (Fig. 2). The alteration of TTs was more prominent after the final wire drawing step (Fig. 2). The $A_f$ decreased from 260 °C to 220 °C and the $M_f$ changed from 170 °C to 120 °C after the 0.75 mm $Ni_{50}Ti_{35}Hf_{15}$ wires were drawn from the 2 mm wires. The decrease of TTs upon hot extrusion and wire drawing (Fig. 2) is associated with the deformation of the material in austenitic state, i.e. so-called ausforming [15]. Both processes were carried out above the $A_f$, and the corresponding formation of dislocation substructures, as well as the resulting structural refinement, further stabilize the austenite [15].

In order to assess the role of the aforementioned processing on the cyclic stability and actuation performance of $Ni_{50}Ti_{35}Hf_{15}$ HTSMA, the thermal cyclic response of the 0.75 mm wire under a constant stress level (300 MPa) was compared with that of the bulk material (Fig. 3). The bulk material exhibited an actuation strain of about 5%, which slightly decreased upon cycling, whereas the 0.75 mm wire exhibited about 3% actuation strain, which remained constant throughout the training. The reduction of the actuation strain in the wire is attributed to the microstructural refinement and possible crystallographic texture in the wire as a result of the relatively high level of deformation upon wire drawing. More importantly, the wire drawing of the $Ni_{50}Ti_{35}Hf_{15}$ HTSMA into a 0.75 wire brought about a more stable actuation response as compared to the bulk material. In particular, the 0.75 mm wire samples exhibited only less than 2% irrecoverable strain in 200 cycles while the bulk material showed more than one order of magnitude higher irrecoverable strain level (more than 25% strain), under the same number of cycles.

Following the training, the martensite start ($M_s$) temperature for the trained 0.75 mm wires was determined as 192 °C, while the $M_s$ was 150 °C for the as-drawn 0.75 mm wires (Fig.2). The $A_f$ of the 0.75 mm wires, on the other hand, remained unchanged (220 °C) upon training, demonstrating that the training significantly decreased the transformation hysteresis ($A_f - M_s$): from about 70 °C to about 28 °C following training. Clearly, training of the $Ni_{50}Ti_{35}Hf_{15}$ wires proved effective in tailoring the hysteresis. The decreased hysteresis is associated with the stabilization of the NiTiHf microstructure by ausforming during hot extrusion and wire drawing, such that further dislocation generation during the transformation is hindered, leading to smaller thermal hysteresis [20]. In addition, the significant improvement in the cyclic stability shown in Fig. 3 is associated with the decrease in temperature

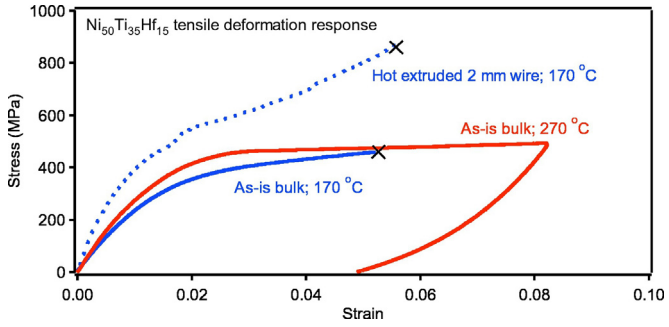


**Fig. 1.** Tensile deformation response of the bulk and hot extruded wire samples of $Ni_{50}Ti_{35}Hf_{15}$ HTSMAs. The black cross at the end of a curve indicates failure of the corresponding sample.

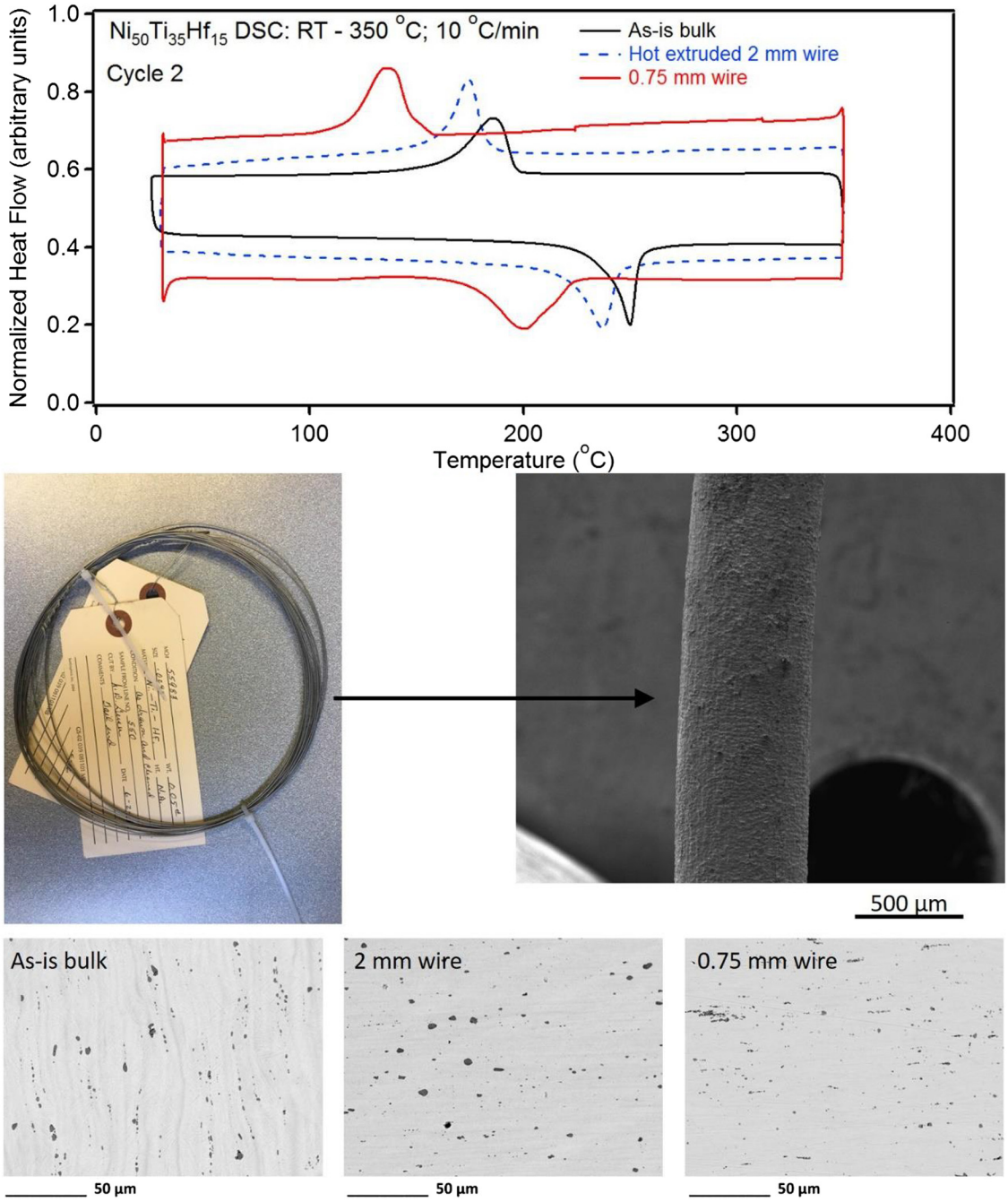


**Fig. 2.** DSC results of the $Ni_{50}Ti_{35}Hf_{15}$ HTSMA, demonstrating the phase transformation behavior of the bulk samples in comparison with the 2 mm diameter hot extruded and 0.75 mm diameter wires (only the second cycles of each DSC analysis is presented). A continuous 12 m long spool of the 0.75 mm wire was obtained upon drawing, and the surface quality was monitored with SEM. The precipitate size and composition were also determined utilizing SEM/EDX.

hysteresis upon cycling, as well as the microstructural refinement and work hardening as a result of the wire drawing, which suppresses extensive plastic deformation accompanying martensitic transformation.

In order to reveal the role of temperature on the deformation response, the $Ni_{50}Ti_{35}Hf_{15}$ wires were deformed to 4% tensile strain at RT, $M_s$ and $A_f$ + 10 °C (Fig. 4) after the thermo-mechanical training shown in Fig. 3. As the test temperature increased, the irrecoverable strain upon unloading decreased significantly, such that near perfect superelasticity was attained at 230 °C in a NiTiHf HTSMA wire for the first time. This trend in irrecoverable strain is expected: the behavior at $M_s$ (192 °C) constitutes martensite reorientation, possibly its small permanent deformation, and the corresponding rubber back effect upon unloading, while the conventional superelasticity is observed above $A_f$. Furthermore, the strength levels decreased significantly when the temperature was increased from RT to $M_s$, due to the role of increasing temperature in enhancing multi-variant martensite formation upon loading. Above $A_f$ (at 230 °C), an almost flat stress plateau was exhibited by the trained wires, and as compared to the bulk material (Fig. 1), despite increasing strength levels, a near perfect superelasticity was attained after the training (Fig. 4). Specifically, dislocations that formed during ausforming and those forming at the phase front during thermo-mechanical cycling are rearranged during the training process, such that only a limited number of new dislocations form upon loading of the trained samples (Fig. 4), where reversible martensitic transformation is not notably interfered with these new dislocations. This is also evident from the very stable phase transformation

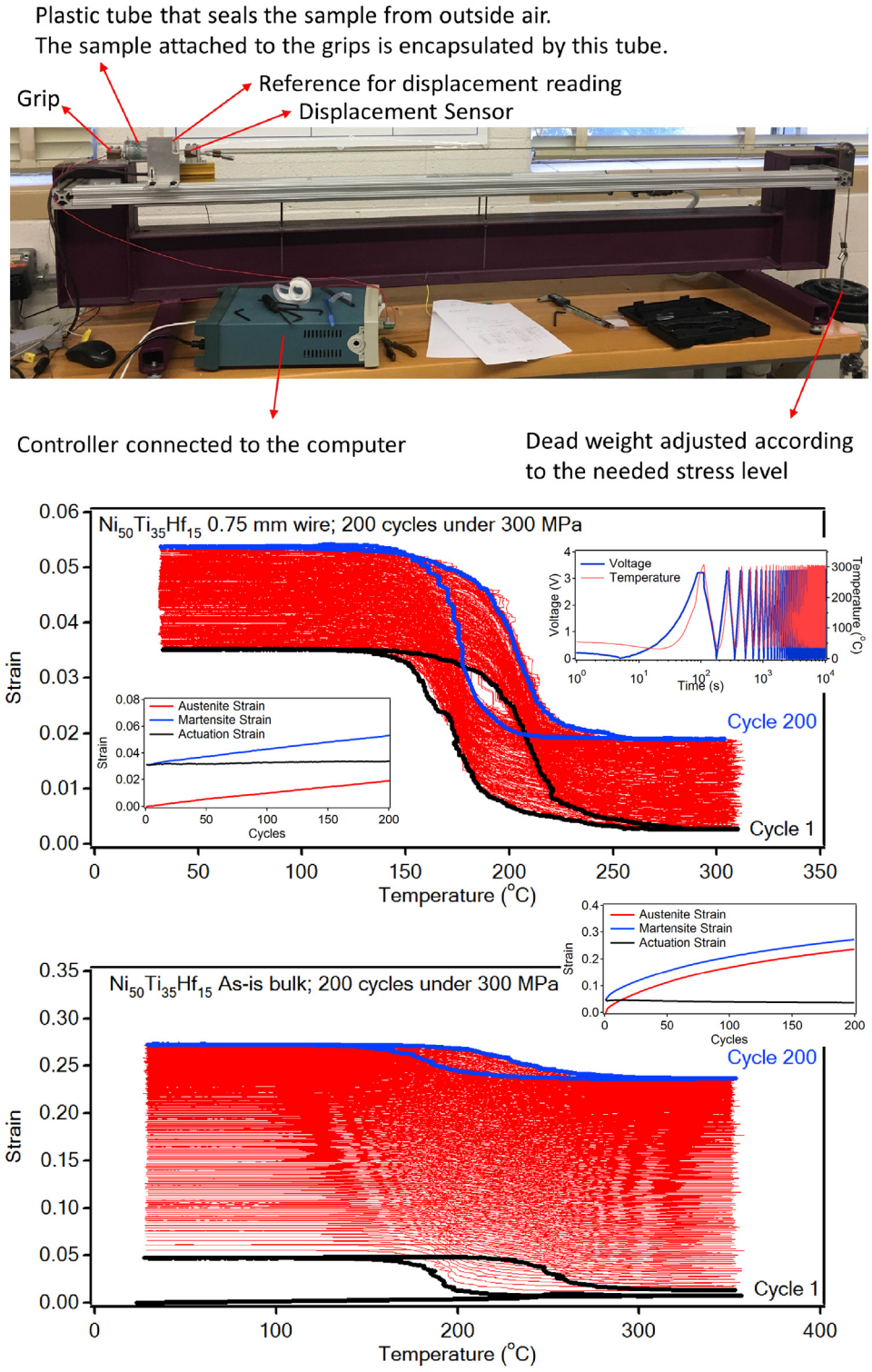


**Fig. 3.** The custom-built wire training setup utilized in the training of the 0.75 mm diameter $Ni_{50}Ti_{35}Hf_{15}$ wires, and the corresponding strain-temperature response of the material during training for 200 cycles under 300 MPa. The insets show the resulting austenite, martensite and actuation strain evolutions (left), as well as the input voltage and the corresponding temperature changes with time (right) throughout the training process. The results of the training on the $Ni_{50}Ti_{35}Hf_{15}$ bulk samples is also provided for comparison. Please note the difference in the y-scales of strain-temperature and strain-cycles plots.

response exhibited by the wires during thermal cycling under constant stress (Fig. 3).

The wire drawing has also improved the ductility of $Ni_{50}Ti_{35}Hf_{15}$ HTSMA as it can be seen by comparing the responses in martensite in Figs. 1 and 4. To better understand the reasons for this improvement, the size and type of the particles in the microstructure have been identified. The particles shown in Fig. 2 was found to be $(Ti,Hf)_2Ni$ precipitates. The average size of the $(Ti,Hf)_2Ni$ precipitates decreased from 3.1 μm to 2.0 μm upon hot extrusion, and further down to 1.8 μm following the drawing, leading to the observed improvement in the ductility in martensite.

Overall, the findings presented herein not only constitute the first set of experimental dataset on the shape memory characteristics of $Ni_{50}Ti_{35}Hf_{15}$ HTSMA wires, in addition to introducing in detail how to

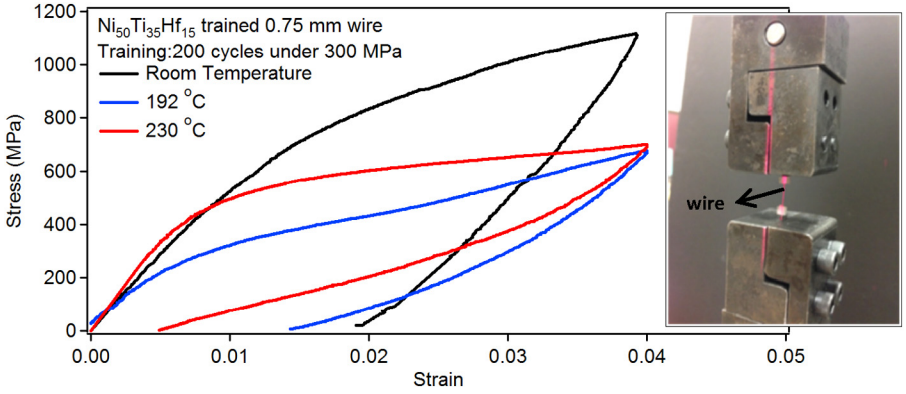


**Fig. 4.** Tensile deformation response of the trained 0.75 mm diameter $Ni_{50}Ti_{35}Hf_{15}$ SMA wires, and the special grips utilized to test the wires at various temperatures.

successfully process NiTiHf wires, but also demonstrate the roles of the test temperature and training on the deformation response of $Ni_{50}Ti_{35}Hf_{15}$ wires. In particular, hot extrusion followed by wire drawing yields an increase in strength levels, yet the brittleness of the bulk material is replaced by near perfect superelastic response above $A_f$. Furthermore, training has proven successful in decreasing the temperature hysteresis and improving the thermo-mechanical cyclic stability, increasing the potential of this HTSMA wires for use in various applications.

## Acknowledgements

The authors acknowledge the financial support by the United Technologies Research Center, through NASA Contract no. NNX15AR27A, and the US Air Force Office of Scientific Research, under Grant no. FA9550-15-1-0287. The SEM and EDX analyses were carried out at Texas A&M University Materials Characterization Facility.

## References

[1] K. Otsuka, C.M. Wayman, Shape Memory Materials, Cambridge University Press, Cambridge, 1999.
[2] J. Ma, I. Karaman, R.D. Noebe, Int. Mater. Rev. 55 (2010) 257–315.
[3] A.M. Pérez-Sierra, J. Pons, R. Santamarta, I. Karaman, R.D. Noebe, Scr. Mater. 124 (2016) 47–50.
[4] X.L. Meng, W. Cai, F. Chen, L.C. Zhao, Scr. Mater. 54 (2006) 1599–1604.
[5] X.L. Meng, W. Cai, Y.D. Fu, Q.F. Li, J.X. Zhang, L.C. Zhao, Intermetallics 16 (2008) 698–705.
[6] H.E. Karaca, S.M. Saghaian, B. Basaran, G.S. Bigelow, R.D. Noebe, Y.I. Chumlyakov, Scr. Mater. 65 (2011) 577–580.
[7] G.S. Bigelow, A. Garg, S.A. Padula, D.J. Gaydosh, R.D. Noebe, Scr. Mater. 64 (2011) 725–728.
[8] O. Benafan, R.D. Noebe, S.A. Padula, R. Vaidyanathan, Metall. Mater. Trans. A Phys. Metall. Mater. Sci. 43 (2012) 4539–4552.
[9] D.R. Coughlin, P.J. Phillips, G.S. Bigelow, A. Garg, R.D. Noebe, M.J. Mills, Scr. Mater. 67 (2012) 112–115.
[10] A. Evirgen, F. Basner, I. Karaman, R.D. Noebe, J. Pons, R. Santamarta, Funct. Mater. Lett. 5 (2012) 1250038.
[11] H.E. Karaca, S.M. Saghaian, G. Ded, H. Tobe, B. Basaran, H.J. Maier, R.D. Noebe, Y.I. Chumlyakov, Acta Mater. 61 (2013) 7422–7431.
[12] O. Benafan, A. Garg, R.D. Noebe, G.S. Bigelow, S.A. Padula, D.J. Gaydosh, N. Schell, J.H. Mabe, R. Vaidyanathan, Intermetallics 50 (2014) 94–107.
[13] A.P. Stebner, G.S. Bigelow, J. Yang, D.P. Shukla, S.M. Saghaian, R. Rogers, A. Garg, H.E. Karaca, Y. Chumlyakov, K. Bhattacharya, R.D. Noebe, Acta Mater. 76 (2014) 40–53.
[14] H. Sehitoglu, L. Patriarca, Y. Wu, Curr. Opin. Solid State Mater. Sci. (2016).
[15] B. Kockar, I. Karaman, J.I. Kim, Y. Chumlyakov, Scr. Mater. 54 (2006) 2203–2208.
[16] S.M. Saghaian, H.E. Karaca, M. Souri, A.S. Turabi, R.D. Noebe, Mater. Des. 101 (2016) 340–345.
[17] R. Santamarta, R. Arróyave, J. Pons, A. Evirgen, I. Karaman, H.E. Karaca, R.D. Noebe, Acta Mater. 61 (2013) 6191–6206.
[18] Y. Wu, L. Patriarca, H. Sehitoglu, Y. Chumlyakov, Scr. Mater. 118 (2016) 51–54.
[19] X.L. Meng, W. Cai, L.M. Wang, Y.F. Zheng, L.C. Zhao, L.M. Zhou, Scr. Mater. 45 (2001) 1177–1182.
[20] A. Evirgen, I. Karaman, R. Santamarta, J. Pons, R.D. Noebe, Acta Mater. 83 (2015) 48–60.
[21] F. Yang, D.R. Coughlin, P.J. Phillips, L. Yang, A. Devaraj, L. Kovarik, R.D. Noebe, M.J. Mills, Acta Mater. 61 (2013) 3335–3346.
[22] C.C. Wojcik, J. Mater. Eng. Perform. 18 (2009) 511–516.
[23] J. Zurbitu, R. Santamarta, C. Picornell, W.M. Gan, H.G. Brokmeier, J. Aurrekoetxea, Mater. Sci. Eng. A 528 (2010) 764–769.
[25] H. Tamai, Y. Kitagawa, Comput. Mater. Sci. 25 (2002) 218–227.
[26] C.N. Saikrishna, K.V. Ramaiah, J. Bhagyaraj, Gouthama, S.K. Bhaumik, Mater. Sci. Eng. A 587 (2013) 65–71.
[27] B. Panton, J.P. Oliveira, Z. Zeng, Y.N. Zhou, M.I. Khan, Int. J. Fatigue 92 (2016) 1–7.
[28] J. Olbricht, A. Yawny, J.L. Pelegrina, G. Eggeler, V.A. Yardley, J. Alloys Compd. 579 (2013) 249–252.
[29] S. Miyazaki, K. Mizukoshi, T. Ueki, T. Sakuma, Y. Liu, Mater. Sci. Eng. A 273–275 (1999) 658–663.
[30] Y.F. Li, X.J. Mi, X.Q. Yin, H.F. Xie, J. Alloys Compd. 588 (2014) 525–529.